J Inorg Organomet Polym (2015) 25:694–701
DOI 10.1007/s10904-014-0147-4

# Syntheses, Structures and Fluorescence Properties of Four Zn/Cd(II) Coordination Polymers with 3-Nitrobenzene-1,2-dicarboxylate and Dipyridyl-typed Coligands

**Gui-lian Li · Guang-zhen Liu · Ling-yun Xin · Xiao-ling Li · Lu-fang Ma · Li-ya Wang**

Received: 10 November 2014 / Accepted: 10 December 2014 / Published online: 16 December 2014


**Abstract** Four new coordination polymers $[Zn(3\text{-}Nbdc)(bpa)]_n$ (**1**), $[Cd(3\text{-}Nbdc)(bpa)(H_2O)]_n$ (**2**), $[Zn(3\text{-}Nbdc)(bpp)]_n$ (**3**) and $\{[Zn(3\text{-}Nbdc)(bpe)]\cdot 1.5H_2O\}_n$ (**4**) (3-Nbdc = 3-nitrobenzene-1,2-dicarboxylate, bpa = 1,2-bi(4-pyridyl) ethane, bpp = 1,3-bis(4-pyridyl)propane and bpe = 1,2-bi(4-pyridyl)ethene), were synthesized hydrothermally and characterized structurally by single crystal X-ray diffractions, elemental analysis and infrared spectroscopy. Complexes **1** and **3** exhibit three-dimensional (3D) metal–organic frameworks with the ($6^6$) dia topology and ($6^5{\cdot}8$) cds topology, respectively, and both of them contain metal-carboxylate helix chains. Compounds **2** and **4** show 2D → 3D interpenetrated networks with (4,4) grid layers and 2D layer, respectively, and both of them contain metal-carboxylate binuclear units. The thermal stabilities and fluorescence properties for complexes **1**–**4** are investigated. The blue-shift of the luminescent wavelength in **2** may be due to the absence of interligand $\pi\cdots\pi$ effects compared with that of other three compounds, but there exist the strong face-to-face $\pi\cdots\pi$ interactions in **1** and edge-to-face $\pi\cdots\pi$ interactions in **3** and **4**, showing a certain degree of interchromophore coupling interaction.

**Keywords** Benzenedicarboxylate · Zinc · Coordination polymer · Helix · Fluorescence

## 1 Introduction

Luminescent coordination polymers are a fascinating class of molecules that have found applications in many areas of chemistry and materials science, where control over the spatial interactions of chromophores represents a significant challenge [1–3]. The geometry of a molecular assembly is often difficult to predict due to the large number of intermolecular forces that can influence the packing of molecules in a crystal. The luminescent coordination polymers with $d^{10}$ metal centers are of great interest due to their higher thermal stability than pure organic materials and the ability to influence the emission behaviors of the organic ligands by the complexation with metal atoms [4, 5]. In contrast to lanthanide coordination polymers typically exhibiting metal ion-centered luminescence [6, 7], luminescence from transition metal polymers is typically centered on the linker rather than on the metal, but can also involve charge transfer between the metal and linker, including ligand-localized emission resulting from the $\pi$–$\pi^*$ and/or $n$–$\pi^*$ transition of conjugated organic molecules, in addition to ligand-to-metal charge transfer (LMCT) and metal-to-ligand charge transfer (MLCT) [8–11].

In the area of transition metal–ligand compounds, the covalent metal–ligand bond distances and angles are frequently discussed as a key on the crystal structures. While hydrogen bonding is now usually pointed out as a packing motif, the possibility of $\pi\cdots\pi$ interactions is mostly not well

**Electronic supplementary material** The online version of this article (doi:10.1007/s10904-014-0147-4) contains supplementary material, which is available to authorized users.

G. Li · G. Liu (✉) · L. Xin · X. Li · L. Ma · L. Wang (✉)
College of Chemistry and Chemical Engineering, Luoyang Normal University, Luoyang 471022, Henan, People's Republic of China
e-mail: gzliuly@126.com

L. Wang
e-mail: wlya@lynu.edu.cn

L. Wang
College of Chemistry and Pharmacy Engineering, Nanyang Normal University, Nanyang 473061, Henan, People's Republic of China

documented in the structure discussion. However, the understanding and utilization of all non-covalent interactions including $\pi\cdots\pi$ stacking is of fundamental importance for the further development of supramolecular chemistry and the tuning and prediction of crystal structures [12–16]. Additionally, the $\pi\cdots\pi$ interaction as an intermolecular force plays an important role in modulating the fluorescent complexes. Related calculations have suggested that the luminescence bandgaps between the highest occupied molecular orbitals (HOMOs) and the lower unoccupied molecular orbitals (LUMOs) can be altered by changing the degree of conjugation in the ligand [17] and also be influenced by the degree of interligand coupling interaction [2]. Face to face $\pi\cdots\pi$ interactions (<4 Å) between the ligands typically show strong intermolecular coupling via $\pi\cdots\pi$ overlap [2, 18]. Non-cofacial chromophore assemblies and those further apart in space (4–8 Å) can show an intermediate degree of coupling, the details of which are significantly dependent on the geometry of the arrangement. Generally, the interligand $\pi\cdots\pi$ interactions can lead to the red shift of the luminescent wavelength [19].

In this paper, we selected a specific Zn(II)/Cd(II)-3-Nbdc system in the presence of various dipyridyl-typed coligands and obtained a serial of four new coordination polymers under similar reaction conditions, namely, [Zn(3-Nbdc)(bpa)]$_n$ (**1**), [Cd(3-Nbdc)(bpa)($H_2O$)]$_n$ (**2**), [Zn(3-Nbdc)(bpp)]$_n$ (**3**) and {[Zn(3-Nbdc)(bpe)]·1.5$H_2O$}$_n$ (**4**). The synthesis, structures, stabilities, and fluorescence for complexes **1**–**4** are given in this paper. For **2**, the obvious blue-shift of the luminescent wavelength may be due to the absence of interligand $\pi\cdots\pi$ effects compared with that of other three compounds, because there exists the face-to-face $\pi\cdots\pi$ interactions in **1** and edge-to-face $\pi\cdots\pi$ interactions in **3** and **4**, showing certain degree of coupling.

## 2 Experimental

### 2.1 Materials and Physical Measurements

All chemicals and reagents were used as received from commercial sources without further purification. Elemental analyses (C, H and N) were determined on a Flash 2000 organic elemental analyzer. Infrared spectra (4,000–600 $cm^{-1}$) were recorded on powdered samples using a NICOLET 6700 FT-IR spectrometer. The thermogravimetric analyses (TGA) were performed on a SII EXStar 6000 TG/DTA6300 analyzer under $N_2$ atmosphere. Powder X-ray diffraction (PXRD) patterns were taken on a Bruker D8-ADVANCE X-ray diffractometer with Cu Kα radiation ($\lambda = 1.5418$ Å). The luminescence spectra were performed on a Aminco Bowman Series 2 luminescence spectrometer at room temperature.

### 2.2 Synthesis of [Zn(3-Nbdc)(bpa)]$_n$ (**1**)

A mixture of $Zn(OAc)_2\cdot 2H_2O$ (0.021 g, 0.10 mmol), 3-$NbdcH_2$ (0.021 g, 0.10 mmol), bpa (0.036 g, 0.20 mmol), KOH (0.006 g, 0.10 mmol) and $H_2O$ (6 mL) was placed in a 23 ml Teflon-lined autoclave, the vessel was heated to 120 °C for 4 days, and then cooled to room temperature. Colorless block crystals were obtained in ca. 82 % yield as a single phase. Anal. calcd (%) for $C_{20}H_{15}N_3O_6Zn$: C, 52.33; H, 3.28; N, 9.21. Found: C, 52.37; H, 3.30; N, 9.16. Selected IR (KBr, $cm^{-1}$): 1616 s, 1592 s, 1528 s, 1459 w, 1427 w, 1353 s, 1220 w, 1157 w, 1066 m, 1033 m, 924 m, 830 s, 776 s, 753 s, 708 s, 671 w.

### 2.3 Synthesis of [Cd(3-Nbdc)(bpa)($H_2O$)]$_n$ (**2**)

The synthetic procedure for **2** was the same as for **1**, except that $Cd(OAc)_2\cdot 2H_2O$ (0.027 g, 0.10 mmol) was used instead of $Zn(OAc)_2\cdot 2H_2O$. Colorless block crystals of **2** suitable for X-ray diffraction were isolated by mechanical separation from the amorphous solid in 75 % yield. Anal. calcd (%) for $C_{20}H_{17}N_3O_7Cd$: C, 45.81; H, 3.25; N, 8.10. Found: C, 45.86; H, 3.27; N, 8.02. Selected IR (KBr, $cm^{-1}$): 3353 w, 1677 w, 1586 s, 1527 s, 1463 w, 1390 s, 1355 s, 1225 w, 1068 w, 1020 m, 927 m, 830 s, 785 w, 753 s, 710 s.

### 2.4 Synthesis of [Zn(3-Nbdc)(bpp)]$_n$ (**3**)

A mixture of $Zn(OAc)_2\cdot 2H_2O$ (0.021 g, 0.10 mmol), 3-$NbdcH_2$ (0.042 g, 0.20 mmol), bpp (0.020 g, 0.10 mmol), KOH (0.006 g, 0.10 mmol), EtOH (3 mL) and $H_2O$ (3 mL) was placed in a 23 ml Teflon-lined autoclave, the vessel was heated to 120 °C for 4 days, and then cooled to room temperature. Colorless block crystals were obtained with ca. yield of 78 % as a single phase. Anal. calcd (%) for $C_{21}H_{17}N_3O_6Zn$: C, 53.33; H, 3.58; N, 8.92. Found: C, 53.35; H, 3.62; N, 8.89. Selected IR (KBr, $cm^{-1}$): 1632 s, 1619 w, 1529 s, 1458 w, 1435 m, 1392 s, 1296 w, 1228 m, 1154 w, 1132 w, 1067 m, 1032 m, 923 m, 820 s, 784 s, 708 s, 667 w.

### 2.5 Synthesis of {[Zn(3-Nbdc)(bpe)]·1.5$H_2O$}$_n$ (**4**)

The synthetic procedure for **4** was also the same as for **1**, except that bpe (0.020 g, 0.10 mmol) was used instead of bpa. Colorless block crystals of **4** suitable for X-ray diffraction were isolated by mechanical separation from the amorphous solid in 65 % yield. Anal. calcd (%) for $C_{20}H_{16}N_3O_{7.5}Zn$: C, 49.69; H, 3.51; N, 8.65. Found: C, 49.66; H, 3.33; N, 8.69. Selected IR (KBr, $cm^{-1}$): 3545 w, 1613 s, 1589 s, 1557 m, 1458 w, 1435 m, 1392 m, 1340 s, 1295 w, 1223 w, 1154 w, 1131 w, 1067 m, 1029 m, 959 m, 923 m, 829 s, 805 w, 785 s, 759 s, 717 s, 659 w.

### 2.6 X-ray Crystallography

The crystallographic data collections for complexes **1–4** were carried out on a Bruker *SMART APEX II* CCD diffractometer equipped with graphite-monochromated Mo $K\alpha$ radiation ($\lambda = 0.71073$ Å) by using the $\varphi/\omega$ scan technique at room temperature. The structures were solved by direct methods with SHELXS-97 and refined on $F^2$ by full-matrix least-squares using the SHELXL-97 program package [20–22]. All non-hydrogen atoms were refined anisotropically and hydrogen atoms were placed in geometrically calculated positions. The details of the structure solutions and final refinements for four complexes are summarized in Table 1. Selected bond distances/angles and hydrogen bonds are listed in Table S1 and Table S2.

## 3 Result and Discussions

### 3.1 Structural Description of $[Zn(3\text{-}Nbdc)(bpa)]_n$ (**1**)

X-ray crystallographic analysis reveals that **1** crystallizes in monoclinic crystal system, space group *C*2/*c* and features a 3D metal–organic framework. The asymmetry unit contains one crystallographically unique Zn(II) atom, one completely deprotonated 3-Nbdc dianion and two half bpa molecules due to their crystallographic special positions, as shown in Fig. 1a. The Zn(II) ion is four-coordinated by two carboxylate O atoms and two bpa N atoms. The Zn–O bond lengths are 1.968 (3) and 2.018 (3) Å, and the Zn–N bond lengths are 2.026 (4) and 2.033 (4) Å, respectively.

The Zn(II) centers are bridged by the 3-Nbdc ligand with two carboxyl groups adopting a monodentate coordination mode to form $2_1$ helix chain along the *b* axis with the Zn···Zn distance of 5.4642 (15) Å, as indicated in Fig. 1b. The opposite chiral helixes occur in an alternate form. There exists the strong face to face $\pi\cdots\pi$ interactions between two benzene rings of 3-Nbdc dianions from the adjacent spiral chains with opposite charials (centroid distance: 3.71 Å, dihedral angle: 0.000°). The adjacent spiral chains are interlinked together through the interchain bpa coligands to form the 3D metal–organic framework (Fig. 1c).

Topological analysis reveals that each Zn center can be regarded as the four-connected network node and both 3-Nbdc and bpa ligands can be considered as 2-connected linkers. Thus, the architecture of **1** can be expressed as dia topology with the Schläfli symbol of ($6^6$) (Fig. 1d).

**Table 1** Crystal and structure refinement data for complexes **1–4**

| | **1** | **2** | **3** | **4** |
|---|---|---|---|---|
| Empirical formula | $C_{20}H_{15}N_3O_6Zn$ | $C_{20}H_{17}N_3O_7Cd$ | $C_{21}H_{17}N_3O_6Zn$ | $C_{20}H_{16}N_3O_{7.5}Zn$ |
| Formula weight | 458.72 | 523.77 | 472.75 | 483.73 |
| Crystal system | Monoclinic | Monoclinic | Tetragonal | Monoclinic |
| Space group | *C*2/*c* | *P*2(1)/*n* | *P*4(1) | *P*2(1)/*c* |
| *a* (Å) | 23.023 (7) | 13.104 (3) | 12.801 (5) | 10.533 (4) |
| *b* (Å) | 8.489 (3) | 11.915 (2) | 12.801 (5) | 22.074 (8) |
| *c* (Å) | 21.864 (7) | 13.995 (3) | 13.355 (9) | 8.632 (3) |
| $\alpha$ (°) | 90 | 90 | 90 | 90 |
| $\beta$ (°) | 118.963 (4) | 100.158 (3) | 90 | 95.740 (4) |
| $\gamma$ (°) | 90 | 90 | 90 | 90 |
| *V* (Å$^3$) | 3,739 (2) | 2,150.9 (7) | 2,188.5 (19) | 1,997.0 (12) |
| *Z* | 8 | 4 | 4 | 4 |
| $D_c$ (g cm$^{-3}$) | 1.630 | 1.617 | 1.435 | 1.609 |
| $\mu$ (mm$^{-1}$) | 1.359 | 1.061 | 1.164 | 1.282 |
| *F* (000) | 1,872 | 1,048 | 968 | 988 |
| $\theta$ range (°) | 2.60–25.50 | 2.60–25.50 | 2.20–25.49 | 2.54–24.99 |
| Reflections collected/unique | 11,934/3,467 | 8,723/3,849 | 12,781/4,000 | 8,089/3,424 |
| *R* (int) | 0.0838 | 0.0358 | 0.0991 | 0.0444 |
| Completeness | 99.3 % | 96.0 % | 99.9 % | 97.4 % |
| Data/restraints/parameters | 3,467/0/271 | 3,849/0/280 | 4,000/1/280 | 3,424/0/289 |
| Goodness-of-fit | 1.038 | 1.041 | 1.046 | 1.020 |
| $R_1$, $wR_2$ [$I > 2\sigma$ ($I$)] | 0.0522, 0.1083 | 0.0413, 0.0896 | 0.0666, 0.1286 | 0.0444, 0.0881 |
| $R_1$, $wR_2$ (all data) | 0.0941, 0.1281 | 0.0666, 0.1005 | 0.1584, 0.1595 | 0.0722, 0.1016 |
| Largest peak and hole (e Å$^{-3}$) | 0.465 and −0.469 | 0.630 and −0.568 | 0.706 and −0.256 | 0.325 and −0.320 |

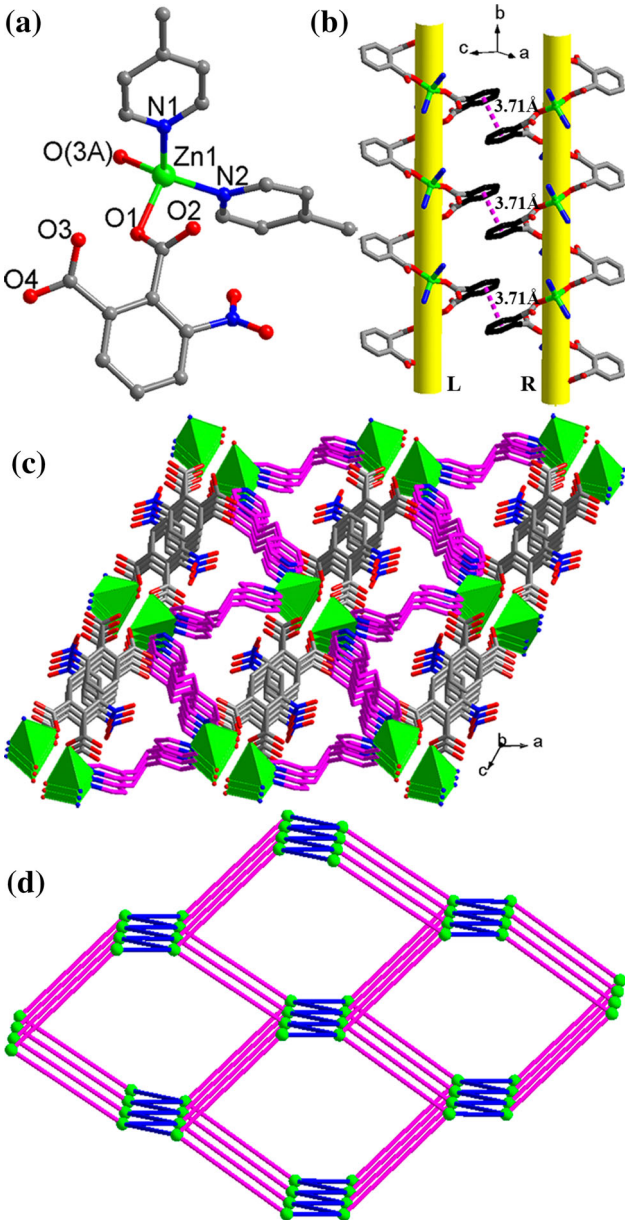


**Fig. 1** **a** View of the coordination environment of Zn atom for **1**. Symmetry codes: A = $-x + 1/2$, $y + 1/2$, $-z + 3/2$. **b** View of 1D helix chain and the face-to-face $\pi\cdots\pi$ interactions between two adjacent helix chain. **c** Polyhedral view of the 3D framework. **d** Topology representation characterized as a monodal 4-*c* net with the dia topology

### 3.2 Structural Description of $[Cd(3\text{-Nbdc})(bpa)(H_2O)]_n$ (**2**)

Complex **2** crystallizes in monoclinic crystal system of *P*2(1)/*n* space group and displays a 2D → 3D interpenetrated structure. The asymmetry unit consists of one crystallographically unique Cd(II) ion, one 3-Nbdc dianions, one bpa molecule and one coordination water molecule. The Cd(II) atom shows a six-coordinated environment with two N atoms from two bpa ligands, three O atoms from two 3-Nbdc dianions, and one O atom from coordination water molecule. All the Cd–O bond lengths are in the range of 2.266 (4)–2.453 (4) Å, and two Cd–N bond separations are 2.283 (4) and 2.336 (4) Å, respectively.

Two adjacent Cd(II) centers are firstly cohered toghether by a pair of 3-Nbdc anions with the bidentate bridging and monodentate coordination modes to form a dimeric unit with the Cd···Cd separation of 5.1278 (8) Å (Fig. 2a). Adjacent binuclear units are cross-linked by bpa coligands along two different directions to result in a 2D layer motif containing rhombic grids with a side length of 17.404/17.711 Å, as shown in Fig. 2b. There exist intralayer H-bonding interactions between coordinated water O atoms and carboxylate O atoms within the binuclear unit (O(7)–H(1W)···O(3): $d = 2.795$ (5) Å, $\theta = 176.1°$; O(7)–H(2W)···O(2): $d = 2.805$ (4) Å, $\theta = 162.4°$) (Table. S2).

Interestingly, there are two sets of parallel 2D layers with the dihedral angle of 82.081°, which are intersperse with each other to result in a 2D → 3D interpenetrated structure (Fig. 2c). In more details, each rhombic grid belonging to one set of parallel layers can permit a pair of layers belonging to another set of parallel layers be interpenetrated. Such type of packing fashion leads to the whole structure with no obvious solvent-accessible volume (Fig. S1).

### 3.3 Structural Description of $[Zn(3\text{-Nbdc})(bpp)]_n$ (**3**)

Compound **3** crystallizes in tetragonal crystal system, space group *P*4(1) and features a 3D metal–organic framework with the Schläfli symbol of $(6^5{\cdot}8)$. The asymmetry unit contains one crystallographic Zn(II) atom, one 3-Nbdc dianion and one bpp molecule (Fig. S2). The central Zn(II) ion is four-coordinated by two carboxylate O atoms and two bpp N atoms. The Zn–O bond lengths are 1.915 (6) and 1.950 (7) Å, and the Zn–N bond lengths are 2.000 (8) and 2.038 (8) Å, respectively.

The Zn(II) atoms are bridged by the 3-Nbdc dianion adopting the bidentate bridging mode to form $4_1$ helix chain along the *c* axis with the Zn···Zn separation of 7.1961 (25) Å, as shown in Fig. 3a. All the helix chains are homochiral with the right-hand feature, so the 3D metal–organic framework belongs to the chiral molecule proved by single X-ray diffraction. The adjacent chains stacked each other through the stronger edge to face $\pi\cdots\pi$ interaction between the phenyl rings of 3-Nbdc anions from adjacent chains, with the C–H···centroid distance of 2.9252 Å, as shown in Fig. 3b (the shortest C···C distance: 3.6277 Å; dihedral angle: 50.49°, as shown in Fig. S3). Previous researches have demonstrated that the electron-withdrawing substituent such as $–NO_2$, $–CF_3$ can obviously improve the stability of the edge to face $\pi\cdots\pi$ interaction [15, 23].

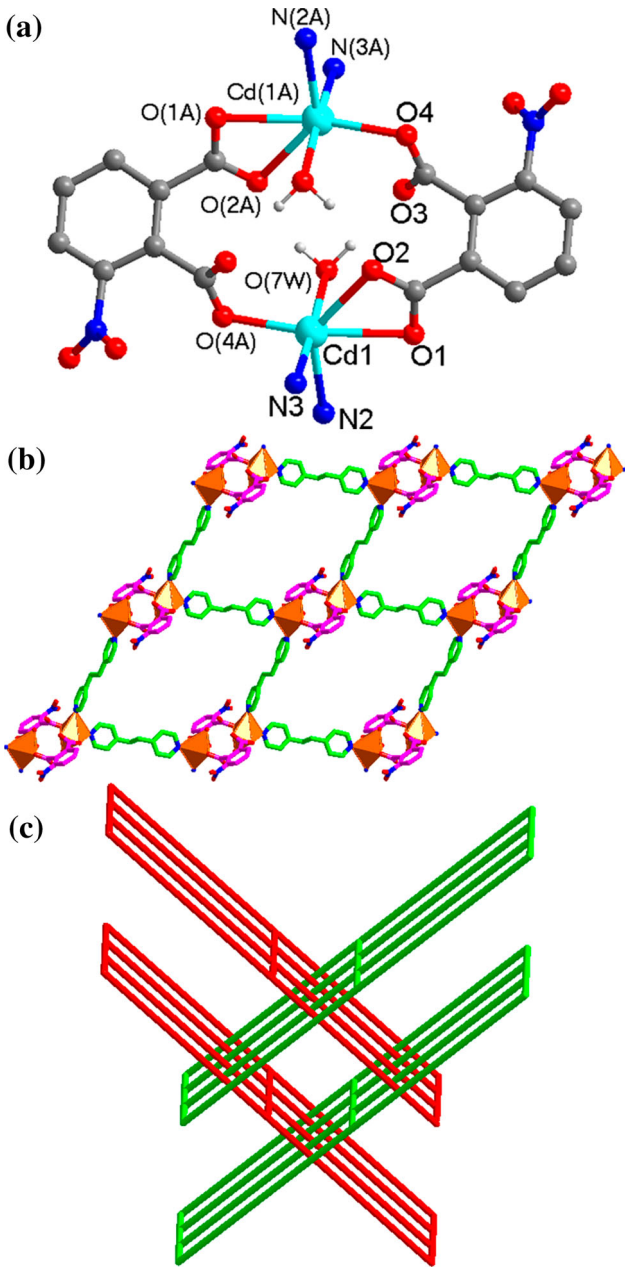


**Fig. 2** **a** View of the coordination environment of Zn atom for **2**. Symmetry codes: A = $-x + 1, -y + 1, -z + 1$. **b** Polyhedral view of 2D layer containing binuclear units linked by bpa coligands. **c** Topology representation displaying the 2D → 3D interpenetrated details

The spiral chains further interlink together by the interchain bpp coligands adopting the tic-tac-toe interpenetration pattern to produce the 3D metal–organic framework with the Zn···Zn distance of 12.8010 (55) Å across bpp ligand. Such dense packing type leads to the whole structure with no obvious solvent-accessible volume (Fig. 3c). Topological analysis reveals that each Zn center can be regarded as the four-connected network node, both 3-Nbdc and bpp can be considered 2-connected linkers. Thus, the architecture of the compound **3** has ***cds*** topology with the Schläfli symbol of $(6^5{\cdot}8)$ (Fig. S4).

### 3.4 Structural Description of $\{[Zn(3\text{-}Nbdc)(bpe)]\cdot 1.5H_2O\}_n$ (**4**)

Compound **4** crystallizes in monoclinic crystal system, space group $P2(1)/c$ and features a 2D layer composed of the binuclear Zn(II) cluster unit, bpe and 3-Nbdc bridging ligands. The asymmetry unit contains one crystallographic Zn(II) atom, one 3-Nbdc dianion, one bpe molecule, one and a half free water molecules, as shown in Fig. 4a. The central Zn(II) ion is four-coordinated by two carboxylate O atoms and two bpe N atoms. The Zn–O bond lengths are 1.953 (3) and 1.961 (3) Å, and the Zn–N bond lengths are 2.021 (3) and 2.058 (3) Å, respectively.

Two Zn(II) neighbours are connected by two 3-Nbdc ligands with both carboxyls adopting monodentate bridging mode forming one dinuclear unit $[Zn_2(OOC)_4N_2]$ with the Zn···Zn separation of 5.0672 (17) Å. The carboxyl-bridged dinuclear units are further extended to produce one 2D coordination polymer lying in the *ab* plane with the Zn···Zn distance of 13.4121 (36) Å across bpe coligands (Fig. 4b). There exists weaker edge to face $\pi\cdots\pi$ interaction between the phenyl of 3-Nbdc anion and pyridyl ring of bpe molecule belonging to two different layers; the shortest C···C distance and dihedral angle are 3.4106 Å and 56.59°, respectively (Fig. S5).

In addition, as a result of the presence of the free water molecules in **4**, there exists the abundant H-bond interactions between the guest waters and carboxylate O atoms of the 3-Nbdc anions (O(8)–H(1W)···O(1): $d = 2.859$ (4) Å, $\theta = 168.9°$; O(8)–H(2W)···O(4): $d = 2.866$ (4) Å, $\theta = 155.4°$; O(9)–H(3W)···O(5): $d = 3.040$ (12) Å, $\theta = 158.0°$; O(9)–H(4W)···O(2): $d = 2.525$ (10) Å, $\theta = 178.9°$) to form its entire 3D supramolecular network (Fig. S6).

### 3.5 Thermogravimetric Analyses (TGA) and Powder X-ray Diffraction (PXRD)

The TGA of **1**–**4** were performed from room temperature to 900 °C under $N_2$ atmosphere, as shown in Fig. 5. The TGA curves of **1** and **3** are very similar with no obvious weight loss from room temperature to 300 °C for **1** and 280 °C for **3**. Upon further heating, their skeletons begin collapse owing to the decomposition of organic ligands. The observed final mass remnant of 17.75 % until 515 °C for **1** and 17.48 % until 700 °C for **3**, likely representing deposition of ZnO, is almost agreement with the calculated value of 17.74 % for **1** and 17.22 % for **3**, respectively. The TGA curve of **2** shows that the weight loss of 3.47 % from 100 to 165 °C is corresponded to one coordinated water per formula unit (calcd: 3.44 %), and the framework

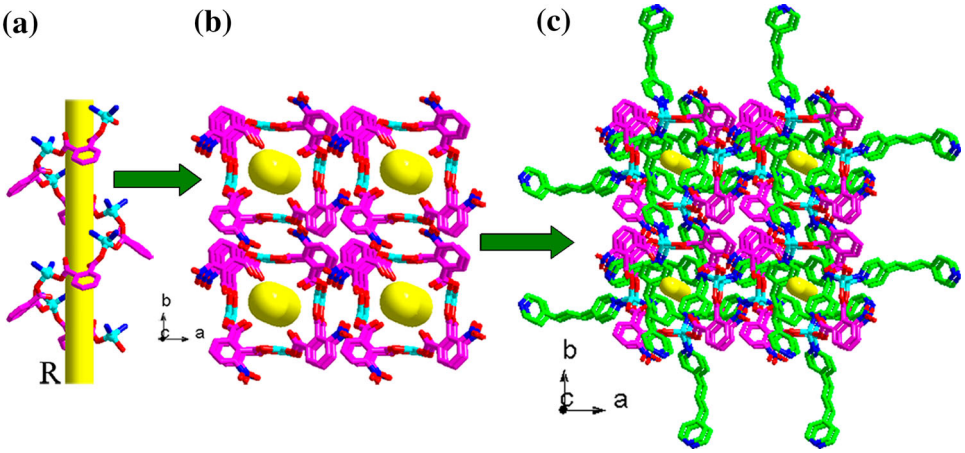


**Fig. 3** **a** View of a 1D right-hand helix chain for **3**. **b** View the stacking of adjacent helix chains. **c** View of the 3D metal–organic framework with 3-Nbdc and bpp as linkers

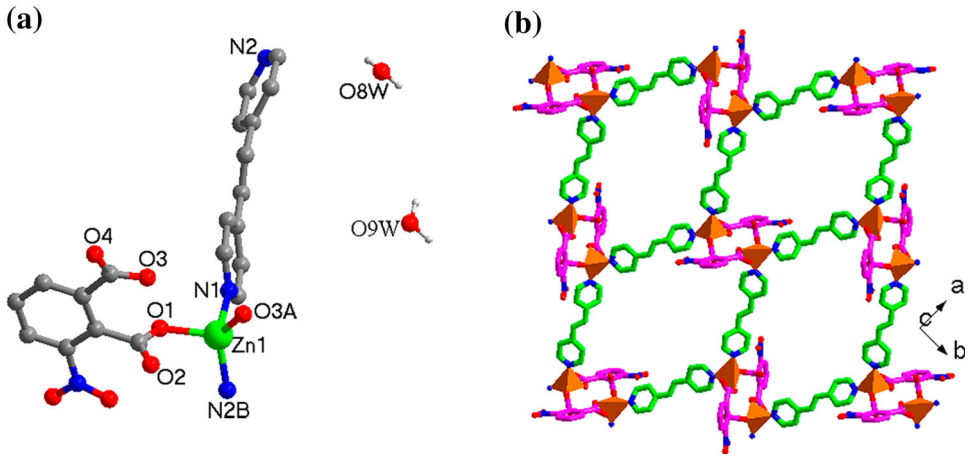


**Fig. 4** **a** View of the coordination environment of Zn atom for **4**. Symmetry codes: A = $-x$, $-y + 2$, $-z + 1$; B = $x-1$, $-y + 3/2$, $z + 1/2$. **b** Polyhedral view of 2D layer containing binuclear units linked by bpe coligands

can keep stability up to 210 °C, then begins a series of weight loss until the heating end owing to the decomposition of organic ligands. For **4**, the first weight loss of 5.56 % from room temperature to 140 °C is attributed to the removal of one and a half free water molecules per formula unit (calcd: 5.58 %). The framework begins to collapse from 275 to 525 °C owing to the decomposition of organic ligands.

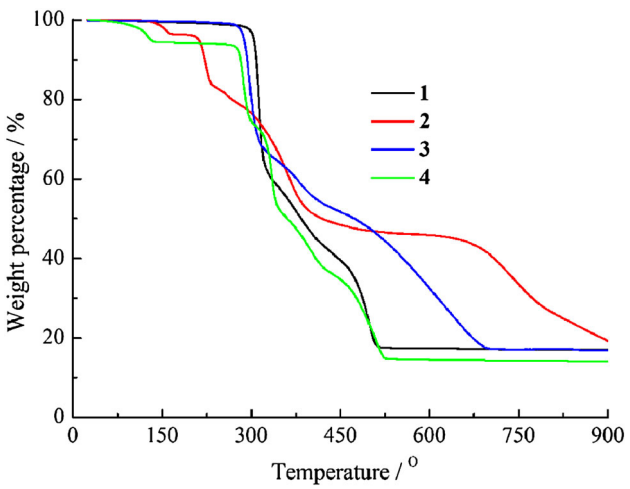


**Fig. 5** The TGA curves for complexes **1**–**4**

The PXRDs of four compounds are in good agreement with the patterns simulated from the respective single-crystal data, implying their good phase purity (Figs. S7–S10).

### 3.6 Photoluminescent Properties

The luminescent properties of coordination polymers with $d^{10}$ metal centers are of great interest due to their highly adjustability upon the coordination of organic ligands. The photoluminescent properties of **1**–**4** and powdered free 3-NbdcH$_2$ ligands were investigated in the solid state at room temperature, as illustrated in Fig. 6. Upon excitation at 298 nm, it is observed that the emission spectra of four complexes are very similar in rough shape, displaying a wide range of the emissions with maximum peaks at ~426 and ~472 nm ($\lambda_{ex}$ = 298 nm) for **1**, **3** and **4** along with ~378 and ~416 nm for **2**. Since the $Zn^{2+}$ and $Cd^{2+}$ ions

are difficult to oxidize or reduce due to their $d^{10}$ configuration, the emissions of all these compounds are neither MLCT nor LMCT in nature. They can probably be assigned to the ligand-centered charge transfer ($n \rightarrow \pi^*$ or $\pi \rightarrow \pi^*$) [24–27] based on 3-$NbdcH_2$ ligand because a similar emission is observed for the free 3-$NbdcH_2$ ligand, whereas the dipyridyl-type coligands show almost no contribution to the emissions of the compounds due to their very weak fluorescent emission in the high energy emission region. The emission spectrum of **1**, **3** and **4** are nearly identical in position to that of the free 3-$NbdcH_2$ molecule, suggesting little contribution from the Zn–O inorganic motifs to the emission and very little degree change of interligand coupling upon metal coordination; in other words, the electronic structures of the coordinated 3-Nbdc anions are not perturbed significantly relative to its free form [28].

The luminescence bandgaps between the HOMOs and the LUMOs can be altered by changing the degree of conjugation in the ligand [17] and also be influenced by the degree of interligand coupling [2]. Face to face stacking (centroid distance: ≤4 Å, dihedral angle: 0.000°) between the organic molecules typically produces strong intermolecular coupling via $\pi\cdots\pi$ overlap [18]. Offset stacking (centroid distance: 3–4 Å, dihedral angle: 0°–10°) [29], edge to face stacking (centroid distance: 4–6 Å, dihedral angle: 30°–90°) [14] can show an intermediate degree of coupling, the details of which are significantly dependent on the geometry of the arrangement. There exists the short cofacial distance of 3.71 Å in **1**, which exhibits strong face-to-face $\pi\cdots\pi$ interactions between the phenyl rings belonging to two adjacent helix chains, showing a high degree of coupling. The aromatic rings in **3** and **4** are appropriate separated meaning intermolecular edge-to-face $\pi\cdots\pi$ interactions in both structures, showing intermediate degree of coupling. Thus compounds **1**, **3**, and **4** display very similar luminescence in emission position. Whereas compound **2** shows obvious blue shift (~50 nm) emissions relative to other three complexes due to the absence of interligand $\pi\cdots\pi$ effects arising a very limited degree of the interchromophore coupling interaction. These results indicate that both the orientation and separation of conjugated linkers have an important influence upon the luminescence spectrum of coordination polymers due to the alterations of spatial and orbital overlap between adjacent aromatic molecules.

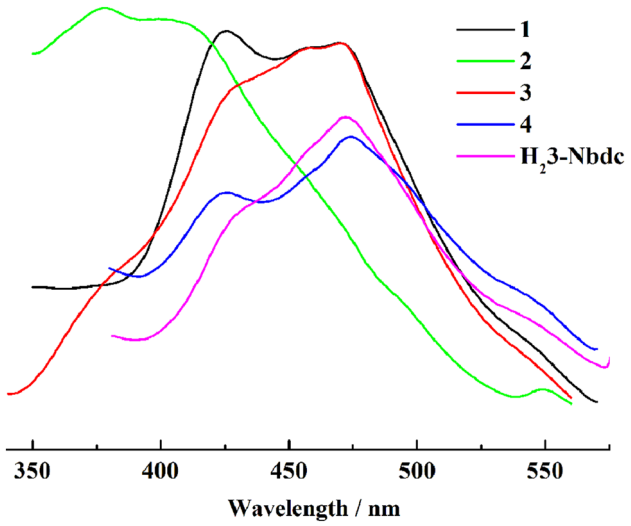


**Fig. 6** The solid-state emission spectra of complexes **1**–**4** and the free 3-NbdcH2 at room temperature

## 4 Conclusions

In summary, four Zn/Cd(II) coordination polymers were successfully synthesized based on 3-nitrophthalic acid and various dipyridyl-typed coligands. Both **1** and **3** exhibit three-dimensional metal–organic frameworks containing metal–carboxylate helix chains. The alternate arrangement of the left- and right-hand $2_1$ helix chains affords the achiral structure for **1**, and the homochiral $4_1$ helix chains produce the chiral structure for **3**. In **2** and **4**, there exist metal-carboxylate binuclear units that are cross-linked by dipyridyl-typed coligands to form (4,4) net motifs. Whereas **2** shows a 2D → 3D interpenetrated networks due to their inclined arrangement between two sets of parallel stacking layers and **4** displays the parallel stacking layers. Furthermore, the solid state luminescence of four compounds are attributed to intraligand $n \rightarrow \pi^*$ or $\pi \rightarrow \pi^*$charge transfer, whereas the obvious blue-shift emission for **2** compared with that of other three compounds can be rationalized by the absence of the interchromophore coupling interaction because of no obvious interligand $\pi\cdots\pi$ effects. It is shown that the luminescence spectrum of coordination polymers is intimately correlated with the ligand environment observed in crystal structures. The studies on their structure–property relationship are very useful for the better understanding of the luminescent mechanism and for the rational designing of photoactive materials, e.g. polymeric light-emitting diodes, in the light of highly adjustable luminescent properties for organic linker upon metal coordination.

## 5 Supplementary Materials

CCDC numbers 1013236-1013239 for compounds **1**–**4**, respectively. These data can be obtained free of charge from the Cambridge Crystallographic Data Center Via http://www.ccdc.cam.ac.uk/data_request/cif.

**Acknowledgments** This work was supported by the National Natural Science Foundation of China (No. 20971064 and 21271098), the Program for Science & Technology Innovation Talents in Universities of Henan Province (No. 14HASTIT017), the Program for Innovative Research Team (in Science and Technology) in University of Henan Province (No. 14IRTSTHN008), and the Foundation of Education Committee of Henan Province (No. 142300410301).

## References

1. M.D. Allendorf, C.A. Bauer, R.K. Bhaktaa, R.J.T. Houka, Chem. Soc. Rev. **38**, 1330 (2009)
2. C.A. Bauer, T.V. Timofeeva, T.B. Settersten, B.D. Patterson, V.H. Liu, B.A. Simmons, M.D. Allendorf, J. Am. Chem. Soc. **129**, 7136 (2007)
3. J. Pang, E.J.P. Marcotte, C. Seward, R.S. Brown, S.N. Wang, Angew. Chem. Int. Ed. **40**, 4042 (2001)
4. U.H.F. Bunz, Chem. Rev. **100**, 1605 (2000)
5. Y.B. Dong, G.X. Jin, M.D. Smith, R.Q. Huang, B. Tan, H.C. Zur, Loye. Inorg. Chem. **41**, 4909 (2002)
6. B.D. Chandler, D.T. Cramb, G.K.H. Shimizu, J. Am. Chem. Soc. **128**, 10403 (2006)
7. D.T. de Lill, N.S. Gunning, C.L. Cahill, Inorg. Chem. **44**, 258 (2005)
8. Z.F. Chen, R.G. Xiong, J. Zhang, X.T. Chen, Z.L. Xue, X.Z. You, Inorg. Chem. **40**, 4075 (2001)
9. M. O'Keeffe, O.M. Yaghi, Science **295**, 469 (2002)
10. G.Z. Liu, S.H. Li, X.L. Li, L.Y. Xin, L.Y. Wang, CrystEngComm **15**, 4571 (2013)
11. L.Y. Xin, G.Z. Liu, X.L. Li, L.Y. Wang, Cryst. Growth Des. **12**, 147 (2012)
12. A. Gavezotti, G. Filippini, J. Am. Chem. Soc. **118**, 7153 (1996)
13. C. Janiak, J. Chem. Soc., Dalton Trans. **21**, 3885 (2000)
14. W.B. Jennings, B.M. Farrell, J.F. Malone, Acc. Chem. Res. **34**, 885 (2001)
15. M.J. Rashkin, M.L. Waters, J. Am. Chem. Soc. **124**, 1860 (2002)
16. E.Y. Lee, S.Y. Jang, M.P. Suh, J. Am. Chem. Soc. **127**, 6374 (2005)
17. B. Civalleri, F. Napoli, Y. Noel, C. Roetti, R. Dovesi, CrystEngComm **8**, 364 (2006)
18. J. Cornil, D.A. dos Santos, X. Crispin, R. Silbey, J.L. Bredas, J. Am. Chem. Soc. **120**, 1289 (1998)
19. G.Z. Liu, X.D. Li, X.L. Li, L.Y. Wang, CrystEngComm **15**, 2428 (2013)
20. G.M. Sheldrick, *A Program for the Siemens Area Detector Absorption Correction* (University of Göttingen, Germany, 1997)
21. G.M. Sheldrick, *SHELXS-97, Program for the Solution of Crystal Structure* (University of Göttingen, Germany, 1997)
22. G.M. Sheldrick, *SHELXL-97, Program for the Refinement of Crystal Structure* (University of Göttingen, Germany, 1997)
23. S.L. Cockroft, C.A. Hunter, K.R. Lawson, J. Perkins, C.J. Urch, J. Am. Chem. Soc. **127**, 8594 (2005)
24. R.B. Fu, S.C. Xiang, S.M. Hu, L.S. Wang, Y.M. Li, X.H. Huang, X.T. Wu, Chem. Commun. **42**, 5292 (2005)
25. X.D. Guo, G.S. Zhu, Q.R. Fang, M. Xue, G. Tian, J.Y. Sun, X.T. Li, S.L. Qiu, Inorg. Chem. **44**, 3850 (2005)
26. G.L. Li, W.D. Yin, G.Z. Liu, L.F. Ma, L.L. Huang, L. Li, L.Y. Wang, Inorg. Chem. Commun. **43**, 165 (2014)
27. G.L. Li, G.Z. Liu, L.L. Huang, L. Li, X. Zhang, J. Inorg. Organomet. Polym. **24**, 617 (2014)
28. S. Bordiga, C. Lamberti, G. Ricchiardi, L. Regli, F. Bonino, A. Damin, K.P. Lillerud, M. Bjorgen, A. Zecchina, Chem. Commun. **20**, 2300 (2004)
29. M.D. Curtis, J. Cao, J.W. Kampf, J. Am. Chem. Soc. **126**, 4318 (2004)